SCIENTIFIC JOURNAL OF MARITIME RESEARCH [POMORSTVO]
University of Rijeka FACULTY OF MARITIME STUDIES

https://doi.org/10.31217/p.38.2.7

A Numerical Study of the Effect of Depth Immersion and Rotation Direction on the Performance of Cross-Flow Savonius Turbines

Dendy Satrio[1*], Dave Johannes Putra[1], Wimala Lalitya Dhanistha[1], I Ketut Aria Pria Utama[1], Teguh Putranto[1], Noorlaila Hayati[1], Maktum Muharja[1], and Madi Madi[2]

[1] Institut Teknologi Sepuluh Nopember, Surabaya 60111, Indonesia
[2] Institut Teknologi Sumatera, South Lampung 35365, Indonesia
[*] Corresponding author, e-mail: dendy.satrio@its.ac.id

ARTICLE INFO

Original scientific paper
Received 5 August 2024
Accepted 10 October 2024

Key words:
Ocean renewable energy
Savonius turbine
Cross-flow
Depth immersion
Rotation direction
CFD

ABSTRACT

Energy supply is a critical variable affecting modern life. Indonesia has many renewable energy sources. One of them is ocean currents. Savonius turbines, which are effective in low-speed currents, have been widely studied in their vertical form, but there has been little progress on cross-flow Savonius turbines. In this study, the turbine performance was investigated in by observing the behaviour caused by the influence of depth immersion, given that the surface of the submersible medium and the surface of the bottom can influence the turbulence. Therefore, the cross-flow Savonius turbine was placed in three different depth conditions: 33%; 50% and 66% of water depth. An analysis was done with Computational Fluid Dynamics (CFD) software. The turbine's rotation direction was also set in two conditions (clockwise and counterclockwise). All these scenarios resulted in the turbine with 66% and the clockwise condition showed the highest results with a Coefficient of power (*Cp*) value of 0.249. The vortices flow pattern created by the clockwise configuration tended downward, in contrast to the counterclockwise which pointed upward. The cross-flow Savonius turbine worked optimally in a low Tip Speed Ratio (*TSR*) where its performance was greatly affected by torque.

1 Introduction

Human dependence on fossil fuels such as oil remains high as a major energy source. With population growth continuing, fuel consumption also rises. By 2023, global oil consumption reached 100.22 million barrels per day, rising from 97.68 million per day in 2022, showing an annual increase of about 2.10% [1]. Oil is a non-renewable energy source and will run out in the future [2], [3], [4] Therefore, research on renewable energy is under way. Alternatives can be taken from a variety of renewable energy sources, including earth heat, wind, the sun, as well as waves and ocean currents.

The kinetic ocean energy from currents is one of the most dominant alternative energy potentials in Indonesia. The majority of Indonesia's regions feature low-speed ocean currents that are ideal for harvesting ocean current energy. These currents typically travel between 0.5 and 1.0 m/s. The current speed can occasionally reach up to 3.0 m/s. However, this is extremely rare [5].

In this context, ocean current turbines become the primary devices for extraction. Various forms of water turbines have been used. Each with its advantages and disadvantages, including the Savonius turbine. The Savonius turbine was created and patented in 1925 by Savonius, a Finnish engineer [6]. The two half-cylindrical blades of the Savonius turbine are arranged in a "S" form. Although it was first intended to convert wind energy, it can also be used to transfer ocean current kinetic energy. There are three varieties of Savonius turbines based on the rotational axis: cross-flow, vertical-axis, and horizontal-axis. Turbines with a vertical axis and cross-flow are appropriate for low current speeds [7], [8].

Several investigations have been carried out to identify factors that influence turbine performance. For example, investigations involving changing the shape of turbine blades to become spirals conducted by Kang et al. [9]. As recommended by Satrio et al. who modified the blade angle to improve self-starting characteristics and manage self-starting from 0.3 to 0.2 m/s [10]. Experiments on turbine array placement have been conducted several researchers, such as Forbush et al. [11] and Bourget et al. [12]. Additionally, Ogawa et al. were able to provide a 14% increase in velocity by changing the shape and geometry of the turbine deflector plates, to improve blade performance [13].

An area of study that remains relatively underexplored and requires attention is the influence of the bottom surface and free surface on real-world application scenarios. The power extracted from the flow may be impacted by a barrier effect brought on by the free surface effect and bottom surface influence [14], [15]. Zhang et al. in earlier research showed that the torque coefficient (*Ct*) rose as depth immersion increased, peaking at an immersion ratio of 1.1 and the *Ct* of 0.7 [15]. This phenomenon is possible because, to preserve mass conservation, the flow inside the channel increases as potential energy decreases, as it does at lesser channel depths. Consequently, the kinetic energy of the flow rises as well. Furthermore, the distance from the turbine to the surface of the water or the seabed can affect the flow around the turbines (wake flow), with the presence of restrictions that can increase the flow above and below the turbine [14].

Another important aspect to consider is the rotation direction of the cross-flow Savonius turbine. Unlike typical turbines such as horizontal and vertical turbines, the performance of a Savonius-type turbine is closely linked to the adjustment of the rotation direction, whether it is clockwise or counterclockwise [16]. As done by Ramadhani et al. [17] revealing that the counterclockwise rotation works optimally for the immersion immersion depth ratio < 0.75, whereas the clockwise works optimally for the immersion ratios ≥ 1.00.

In a previous study Golecha et al. had done research on a Savonius turbine but in a vertical laying, or vertically straight with the bottom surface [18]. Therefore, in this study the Savonius Turbine was be placed with a cross-flow configuration as a refreshment point to obtain a more complete coverage of insights related to the Savonius turbine with its parameters. For these reasons, this study utilized CFD simulations to analyze the effects of immersion depth and rotational direction on turbine performance, focusing on key performance parameters such as *Cp*.

2 Material and Methods

2.1 Turbine Geometry and Study Variations

This study was inspired by some previous studies, but it utilized a slightly different technique [18]. The purpose of this study was to determine the immersion depth and rotation direction of the performance produced by a Savonius turbine. The turbine geometry of the research conducted by Golecha was adopted and modified to match the CFD simulation, thus obtaining the parameters of Savonius turbines to be used in detail as shown in Table 1.

In addition to variations in the immersion depth, the rotation direction of the turbine is also divaricated by referring to the clockwise and the counter-clockwise rotation direction as shown in Figure 1.

The turbine was placed at three different immersion depth variation: 0.817 meters (33%), 1.225 meters (50%), and 1.633 meters (66%). Long-term considerations in determining variations in the depth of immersion included significant non-technical factors.

Previously, Ramadhani et al. conducted similar studies with detailed variations in immersion depth, ranging from an immersion ratio of Z/D = 0.25 to Z/D = 3 [17]. In their study, Z/D was the same parameter as *dh* shown in Figure 1, where Z/D represented the ratio of the distance from the free surface to the turbine center over its diameter.

Table 1 Turbine parameters and specifications.

Parameters	Specifications
Turbine type	Savonius turbine
Axis type	Vertical → cross-flow
Turbine diameter (D)	0.245 m
Turbine length or span (S)	0.170 m
Blade thickness (t)	0.002 m
Number of blades (N)	2
Water depth (H)	2.45 m
Depth immersion (d_H)	33%, 50% and 66%
Rotation direction	Clockwise & counterclockwise

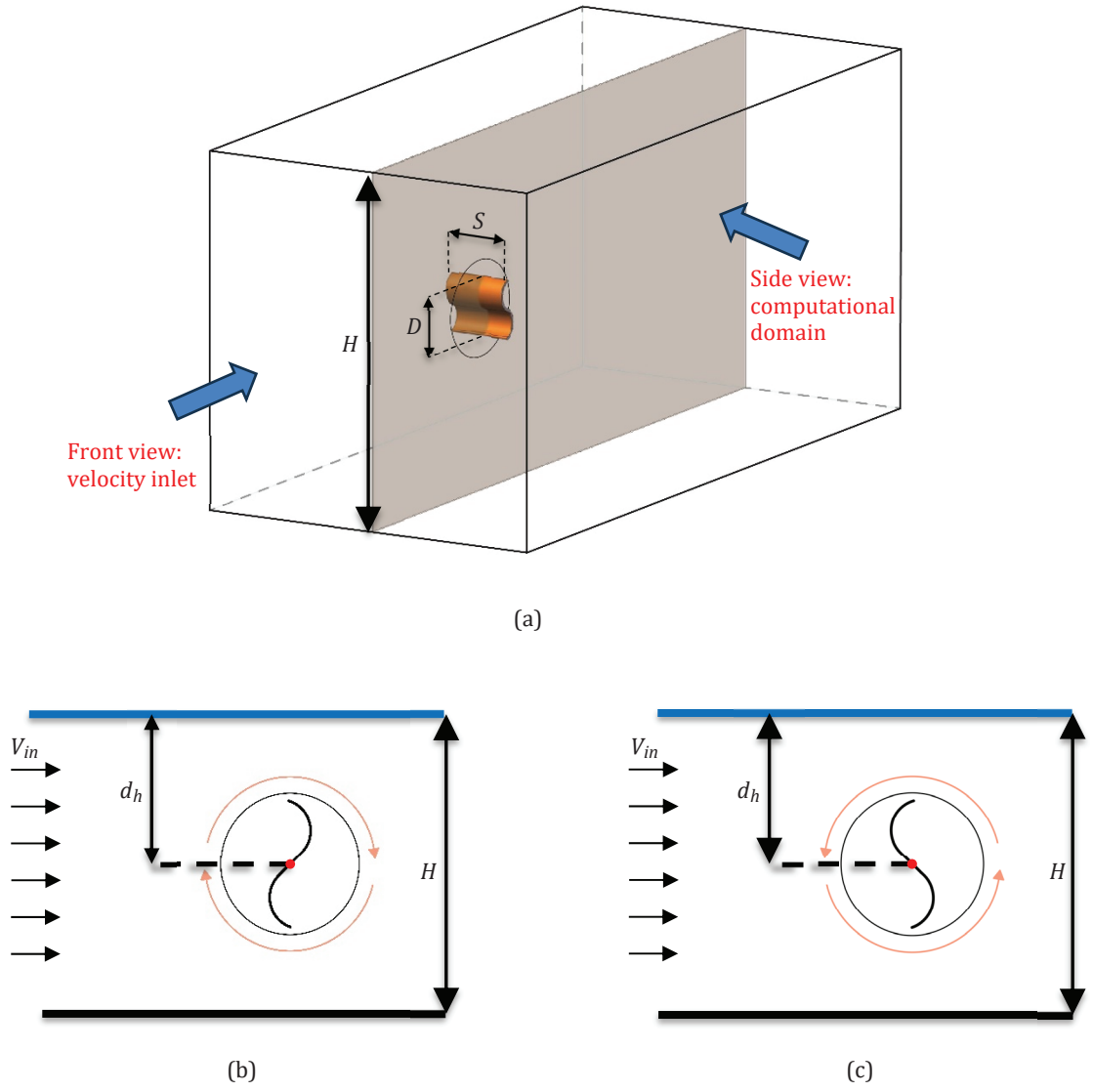

Figure 1 Design parameters in cross-flow Savonius turbine (a) with (b) clockwise and (c) counterclockwise rotational direction.

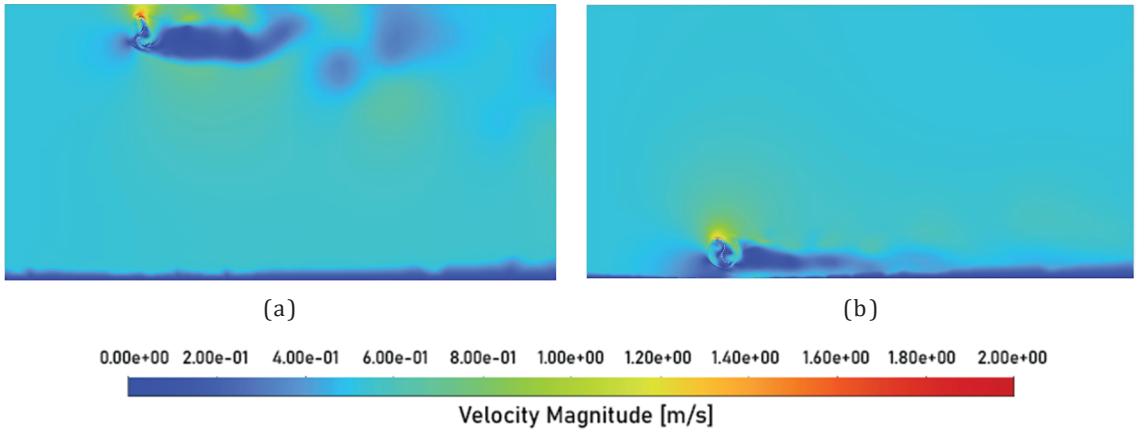

Figure 2 Flow visualization of the turbine interaction with (a) sea surface and (b) seabed.

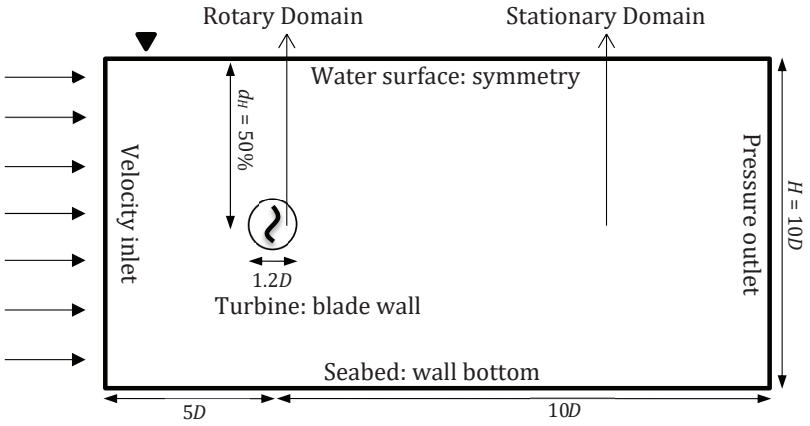

Figure 3 Computational domains and boundary conditions.

However, in this study, additional limitations were set in determining the immersion depth variation, by adopting the recommendations for the installation of marine structures from the European Marine Energy Centre (EMEC). The EMEC recommends that the turbines and their structures be installed at least 5 meters below the water surface, and have a minimum distance of 25% from the seabed under the Lowest Astronomical Tide conditions (LAT) [19].

The distance from the water surface was intended to avoid collisions with ships, fishing boats, and other activities. Setting a minimum distance from the seabed aimed to prevent damage to the turbine body from debris and hard materials carried by the currents along the sea floor. Figure 2 shows the intense interaction between the turbine and both the water surface and the seabed. When the turbine was placed close to the sea floor, as shown in Figure 2 (b), the currents directly swept the sea bottom. If there is hard material in the flow, it is highly likely to damage the body. Similarly, a turbine located near the surface, as shown in Figure 2 (a), is also at risk.

2.2 Computational Domains and Boundary Conditions

The computational space was used to represent the turbine and all its immersion depth variations. As shown in Figure 3. The rotational domain served as a turbine, where this domain had a magnitude of 1.2*H* to give space to the blades, while the stationary domain functioned as a fluid that moved through the turbines, so the domain was divided into two zones. Between these two zones there were interfaces of each zone as boundaries and connectors. In addition, the rotation speed of the rotational domain became the input.

The simulation model of such a turbine was placed in the cross-sectional area, with each parameter referring to the diameter interval of the turbine. The medium used as a fluid had a length of 20*D* (4.9 meters) and a width of 10*D* (2.45 meters), as shown in Figure 3. The position of the turbine along the X-axis was not exactly in the center of the medium but it was located at a position of 5*D* from the nearest side, leaving a distance of 15*D* from the other side. This arrangement allowed for a more comprehensive observation of the fluid behaviour that occurred after passing through the turbine.

Additional boundary condition settings were applied, such as setting the turbine blades and 'bottom_wall' to a wall configuration, with the default parameters from Ansys Fluent where the roughness constant was 0.5 and the roughness height was 0. The direction and fluid velocity was specified regarding the "*inlet*" section at a velocity of 0.54 m/s. Fluid led to the "*outlet*" section because that section was defined as the direction of the outflow with a configuration with symmetric boundary conditions. The size of the domain behind the turbine was considered sufficient to accommodate the wake effect that was generated, as shown in Figure 3 [20]. This prerequisite referred to previous research experience conducted by Satrio et al. [21].

2.3 A Grid Independence Study

Firstly, to determine the appropriate number of mesh components, mesh independence research was conducted. At a velocity inlet of 0.54 m/s, the turbine was studied without any flow disruption. Figure 4 displays the results of the mesh independence study. The analysis started with 73,000 mesh components and progressively increased to 783,000 elements to evaluate the effect of mesh refinement on the performance of the turbine by analyzing its torque. As the number of elements increased, the results were monitored for consistency, ensuring that further refinement did not significantly affect the outcomes.

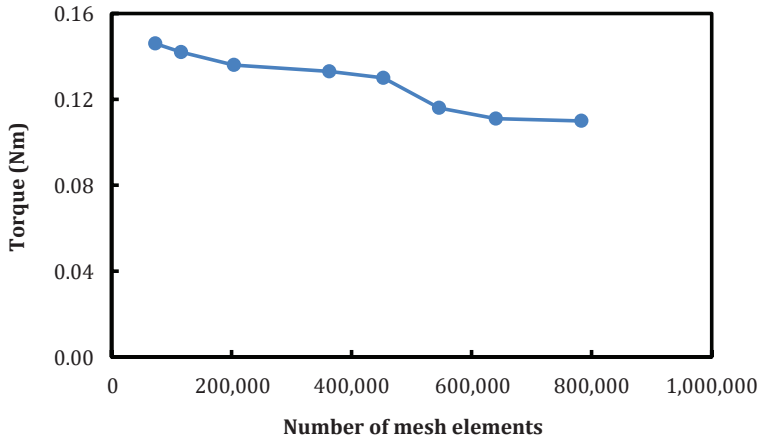

Figure 4 A grid independence study for the cross-flow Savonius turbine.

A stable torque value was achieved with 640,511 elements, confirming that further increases in the mesh had minimal impact on accuracy. However, adding more elements significantly extended the computation time, making the process less efficient. For practical reasons, we rounded the mesh count to 641,000 elements, ensuring both accuracy and computational efficiency.

Second, obtaining good simulation results also depended on mesh quality. Unstructured mesh was used throughout the entire mesh. As shown in Figure 5, the

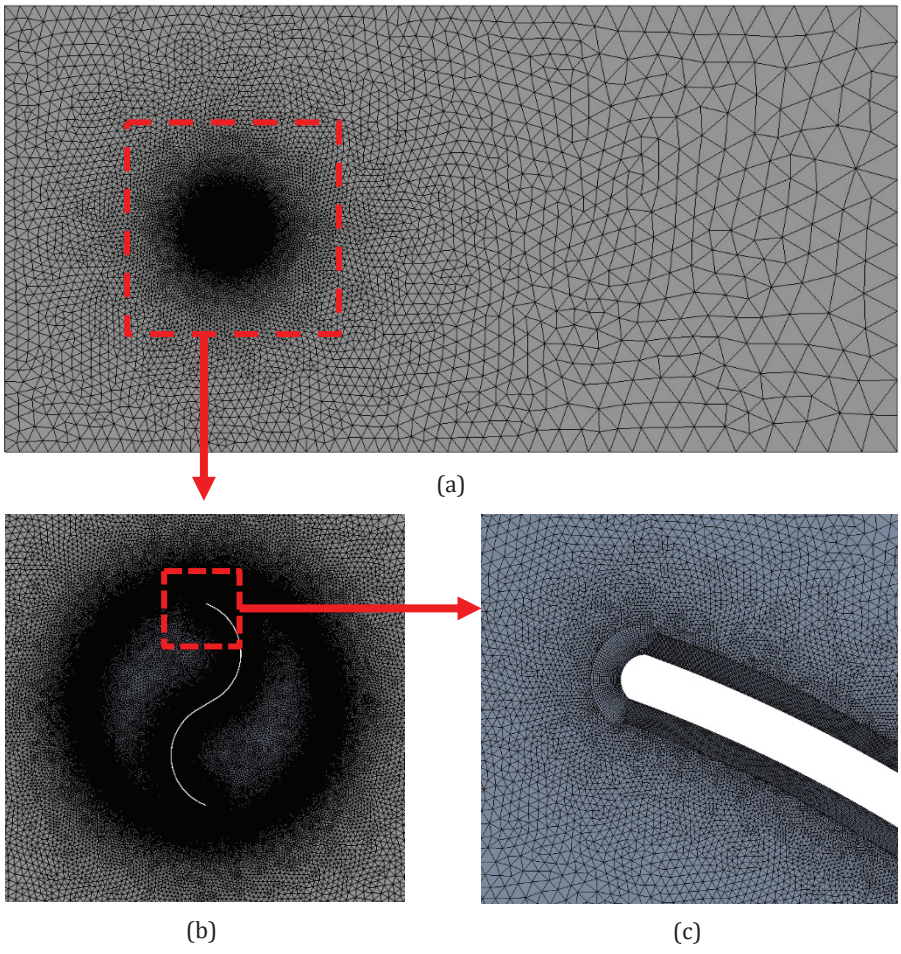

Figure 5 Meshing strategy on the computational domain: (a) overall geometry, (b) near the turbine, and (c) inflation on the blade wall.

mesh components were dispersed from the central turbine to the fluid domain. After that, as illustrated in Figure 5 (b and c), the mesh near the turbine was fine-tuned. Additionally, layers were inflated in the blade wall to address the boundary layer flows [22]. The simulation employed the K-ω SST turbulence model, which performed computations accurately in the regions of the bulk and boundary-layer due to low Reynolds number operation of the turbine [23]. The value of $y+ < 1$ had to be adjusted when using K-ω SST.

2.4 The Number of Rotation Studies

The number of turbine rotations affected the number of time steps required in the calculations. More rotations result in more time steps needed. This impacted the overall computation time. According to studies conducted by Satrio et al. [10], a minimum of four rotations is necessary for accurate calculations, as this allows the wake to fully develop. The first rotation (0^0-360^0) showed some fluctuations, indicating that the average torque during this period may not be representative. Although the second and third rotations appeared to be more stable, the wake was still forming and remained close to the turbine. By the fourth rotation ($1{,}080^0$-$1{,}440^0$), the wake was fully developed. This provided a reliable parameter for validation. The moment coefficient for each rotation is illustrated in Figure 6 below.

In Table 2 below, comparing the average torque generated for each rotation, it was evident that there was still an error in the first rotation compared to the second rotation. After the second rotation, the generated torque stabilized and showed no significant differences. Of all the turbine revolutions, the smallest error was obtained in the 6th revolution with a value of 0.73%.

2.5 Solver Settings and Performance Parameters

A sliding mesh approach under transient settings was used in the simulation. The K-ω SST turbulence model was based on reference [23]. The fluid was defined as water (H_2O), and the turbine blade was set up as a wall using the default material. The simulation was solved using the Unsteady Reynolds Averaged Navier-Stokes (U-RANS) equation. There was a one-time step size (TSS) of 5˚. Additionally, because of its steady state, six turbine rotations were used. Before introducing alterations in the immersion depth and rotation direction, the output simulation was verified through experimental data collection. After that, the performance of the turbine was evaluated based on predetermined performance criteria.

$$Ct = \frac{Torque}{0.5\rho V^2 AR} \tag{1}$$

$$TSR = \frac{\omega R}{V} \tag{2}$$

$$Cp = Ct \cdot TSR \tag{3}$$

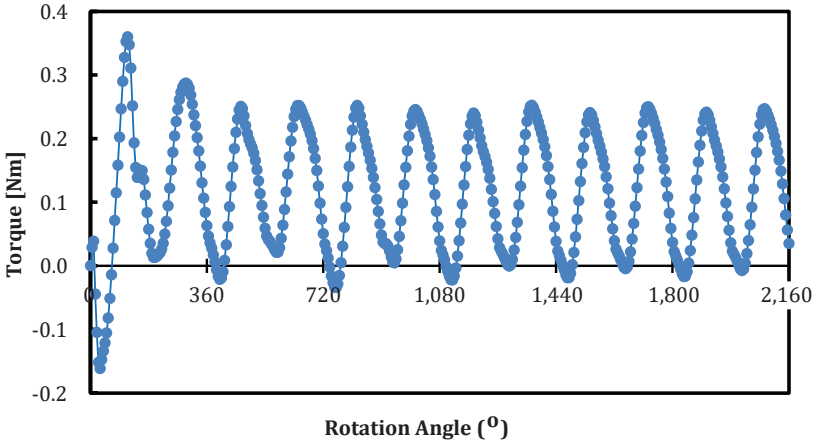

Figure 6 Torque fluctuations regarding the angular position of the turbine rotation.

Table 2 The average value on each rotation and its percentage error.

Rotation	1st	2nd	3rd	4th	5th	6th
Torque (Nm)	0.119	0.126	0.117	0.116	0.116	0.115
Ct	0.298	0.314	0.292	0.288	0.289	0.286
Cp	0.220	0.232	0.216	0.213	0.213	0.212
Error (%)	-	5.20	7.64	1.24	0.09	0.73

The numerical simulation provided time series data measuring the torque [Nm] of a cross-flow Savonius turbine. This torque data is converted into the Coefficient of torque (*Ct*) using Equation (1). Equation (2) was utilized to calculate the Tip Speed Ratio (*TSR*) or was known as a comparison of the turbine's angular speed and input velocity (*V*). By integrating Equations (1) and (2), the Coefficient of power (*Cp*) was derived, as shown in Equation (3). The variables *R, A* and ω represent the turbine radius, swept area, and rotational speed, respectively. Whereas ρ is the density of the fluid used in the simulation (water liquid) with a value of 997 Kg/m^3.

3 Results And Discussion

3.1 Numerical Validation and Axis Configuration

Experimental data published from previous studies were used to validate the original turbine that had not applied its immersion depth and rotation direction variations. The simulation was done with the *TSR* settings 0.7, 0.74, 0.8, 0.86, 0.9, 0.98, 1.015, 1.068, and 1.086, where these *TSR* sets were the same as those performed in the study for validation. The CFD calculation results in a torque [Nm] that was then processed using Microsoft Excel to obtain torque and *Ct* values. Next, *Cp* was calculated from the torque by meeting the (3) equation described earlier. It is important to know that the research utilized as a validation benchmark uses a vertical turbine, so this validation process utilized a vertically positioned turbine, which was then rearranged to meet a horizontal axis so that it became a cross-flow turbine. Here are the results of the validation between the reference research as validation and the simulation carried out.

The *Ct* and *Cp* values in Figures 7 and 8 exceeded the intended error rate of 10%, with errors surpassing 29%. This discrepancy likely stemmed from using three-dimensional reference data while conducting two-dimensional simulations, which could lead to overestimation [24]. Additionally, the unstable conditions during rotor operation suggested a need for further time and spatial sensitivity analysis [24]. Despite these issues, the graphical trends of the simulation showed a relatively stable error percentage, indicating acceptable performance.

As described earlier, the next step was to modify the turbine by changing its axis orientation, shifting from the Z-axis to the X-axis, thus converting it from a vertical to a cross-flow turbine configuration. There were some dif-

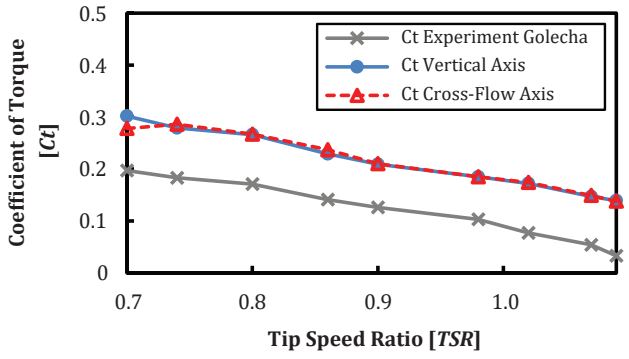

Figure 7 Numerical validation of torque coefficient for vertical axis and cross-flow axis configurations against Golecha experimental data [18].

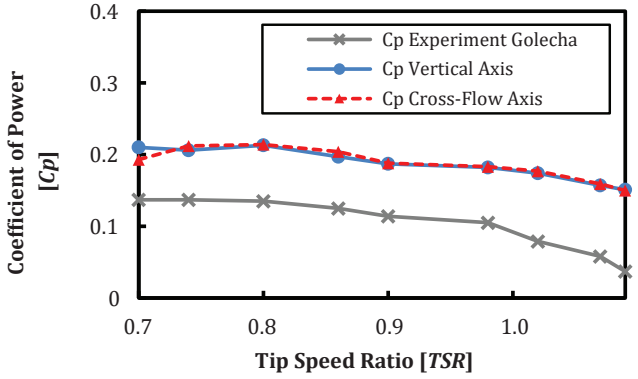

Figure 8 Numerical validation of power coefficient for vertical axis and cross-flow axis configurations against Golecha experimental data [18].

ferences in the configuration between a vertical and a cross-flow, incorporating the seabed "*wall_bottom*" as a no-slip wall and gravity into the CFD software. The value that resulted from adding these configurations matched the cross-flow and the vertical turbines. Comparisons between the outcomes of the two CFD numerical simulations on vertical and cross-flow turbine layouts are displayed in Figures 7 and 8 above. When the results of the two simulations were compared, the value trends for the cross-flow turbine and the vertical turbine configuration showed only slight differences. This suggested that both turbine types performed similarly under the same conditions, although the vertical turbine tended to achieve slightly better results in certain parameters. The *Cp* produced by a vertical turbine had outperformed the cross-flow at *TSR* 0.7 and 1.086. This explained that why the cross-flow turbines were been slightly better than vertical turbines [25]. As a result of this comparison, the next step in the study was to apply variations in immersion depth and rotation direction to further evaluate the performance differences between the two turbine types.

3.2 Effect of the Turbine Depth Immersion

Considering various factors, this study did not select immersion depths too close to the surface or the seabed. Therefore, the immersion depth variations used were 33% (0.8167 m), 50% (1.2250 m), and 66% (1.6333 m). This selection aimed to explore different effects on turbine performance without disrupting the flow of the turbine caused by free surface or seabed disturbances. The depth of the water was 2.45 m. The three diving distances were selected to determine the performance of cross-flow turbines at depths close to the surface of the water to the bottom of the sea. By applying equations 1, 2 and 3 to find out the values of *Ct, Cp* and *TSR*, the cross-flow performance of the turbine was evaluated at each immersion depth. Here are the results obtained from the simulations.

Figures 9 and 10 suggest that the 50% immersion depth, marked by the red line, might be in a zone that reduced interaction with both the surface and seabed, indicating a potentially more stable condition.

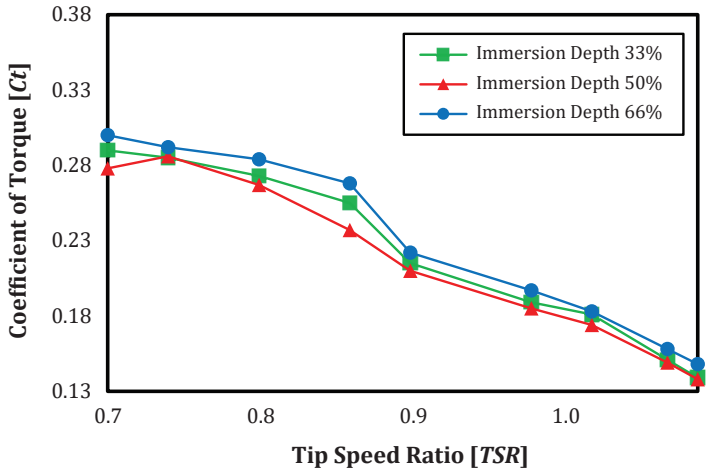

Figure 9 The influence of depth immersion regarding torque coefficient of cross-flow Savonius turbine.

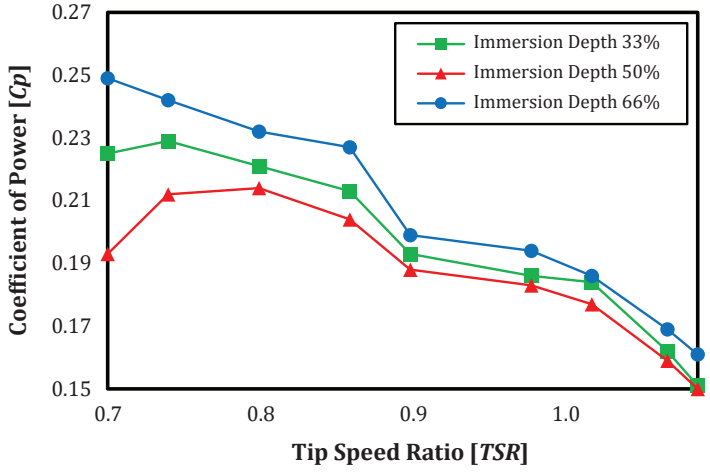

Figure 10 The influence of depth immersion on power coefficient of cross-flow Savonius turbine.

However, this depth delivered the poorest performance compared to other variations. For example, this variation could only reach a maximum *Cp* of 0.214 on a *TSR* of 0.8 whereas on the same *TSR* the variation of 66% could reach a value of 0.232 and the variance of 33% might reach 0.221. The same results were true of the value as shown in Figure 9 since the trend shown remained consistent.

This happened because a Savonius turbine uses drag force to operate, unlike horizontal and vertical turbines that generally operate using lift force [7], [26]. The fluid interaction with the two surfaces allows for a flow disruption before passing through the turbine blade, which can turn the flow into turbulent thereby enhancing the drag style. The influence of the kinetic force of water also needs to consider the selection of the material type [27], [28] and the strength of the turbine structure [29]. Therefore, it is not surprising that the drag style that comes up does not give a decrease in performance and vice versa. This is in line with the research results revealed by Ramadhani et al. stating that where depths of immersion closer to the base tend to yield better results [17]. This can also be observed in Figures 9 and 10 showing that the linear performance decreased with an increase in *TSR*. The most insignificant decline was seen in the *TSR* 0.9 where the immersion depth variation of 66% had a 12% decreased *Cp* value from 0.227 to 0.199, the 50% variation had a 13% decline from 0.213 to 0.199, and the latter, 33% variance, had an 8% decrement from 0.204 to 0.188. After such a significant decrease, the *Ct* and *Cp* values consistently underwent periodic decreases. This finding provided the fact that the Savonius turbine worked optimally at low *TSR*.

In Figures 11 (a) and (b), *Cp* values at low and medium *TSRs* consistently fell below *Ct* values, with the average *Cp* at low *TSR* approximately 26.2% lower than *Ct* and an 11% difference at medium *TSR*. In contrast, Figure 11 (c) shows that *Cp* exceeded *Ct* by 7.97% at higher *TSRs*. These findings suggested that torque significantly impacted the performance of the Savonius crossflow turbine at low to medium *TSRs*, while performance at high *TSRs* was mainly driven by rotational speed.

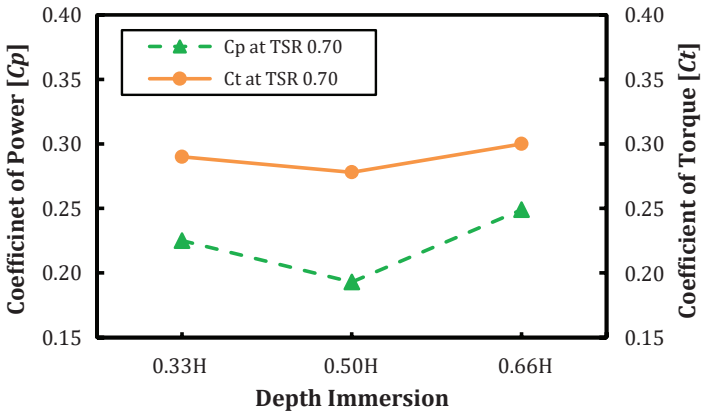

(a) Lower*TSR*

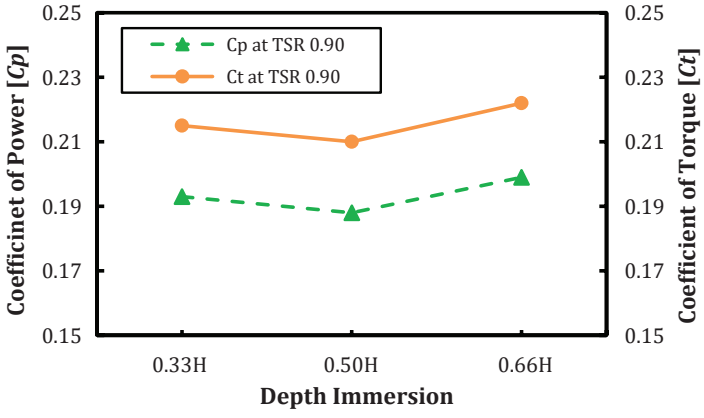

(b) Medium*TSR*

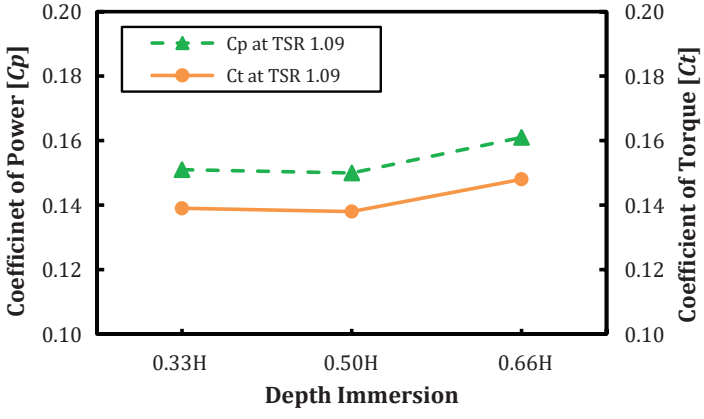

(c) Higher*TSR*

Figure 11 Comparison of *Cp* and *Ct* values on (a) lower *TSR* 0.70, (b) medium *TSR* 0.90, and (c) higher *TSR* 1.09.

3.3 Effects of the Turbine Rotation Directions

The turbine rotation is configured as described in Figure 1 for all points and immersion depth variations. Accordingly, the direction has been modified to counterclockwise.

The counterclockwise configuration generally produces improvements like the 33% variation where the clockwise configuration gets a maximum value on the 0.74 *TSR* by 0.229 and increases to 0.242, or an increase of 6% on the counterclockwise configuration. Likewise, the 50% variance where the clockwise configuration got the highest *Cp* value at 0.8 *TSR* with a reach of 0.214, increased in the counterclockwise configured to 0.223 or increased by 4%. However, a different pattern of improvement occurred in the 66% variance, where the counterclockwise configuration instead showed a decrease where the maximum *Cp* of the 0.7 *TSR* decreased from 0.249 to 0.233 or a recorded decline of 6%. This is an interesting finding, so the count of each variation is presented in Figure 12 to underline a more comprehensive analysis.

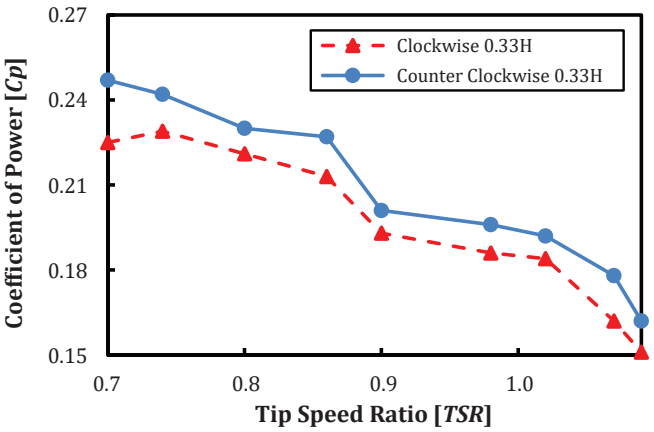

(a) Immersion Depth 33%

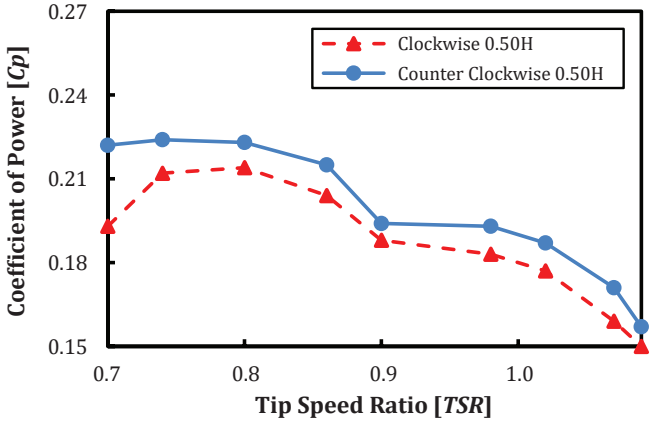

(b) Immersion Depth 50%

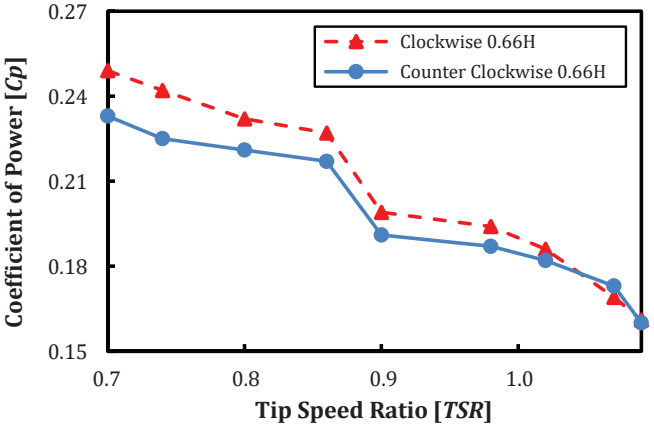

(c) Immersion Depth 66%

Figure 12 The influence of rotation directions regarding the power coefficient of cross-flow Savonius turbine on depth immersion of (a) 33%, (b) 50%, and (c) 66%.

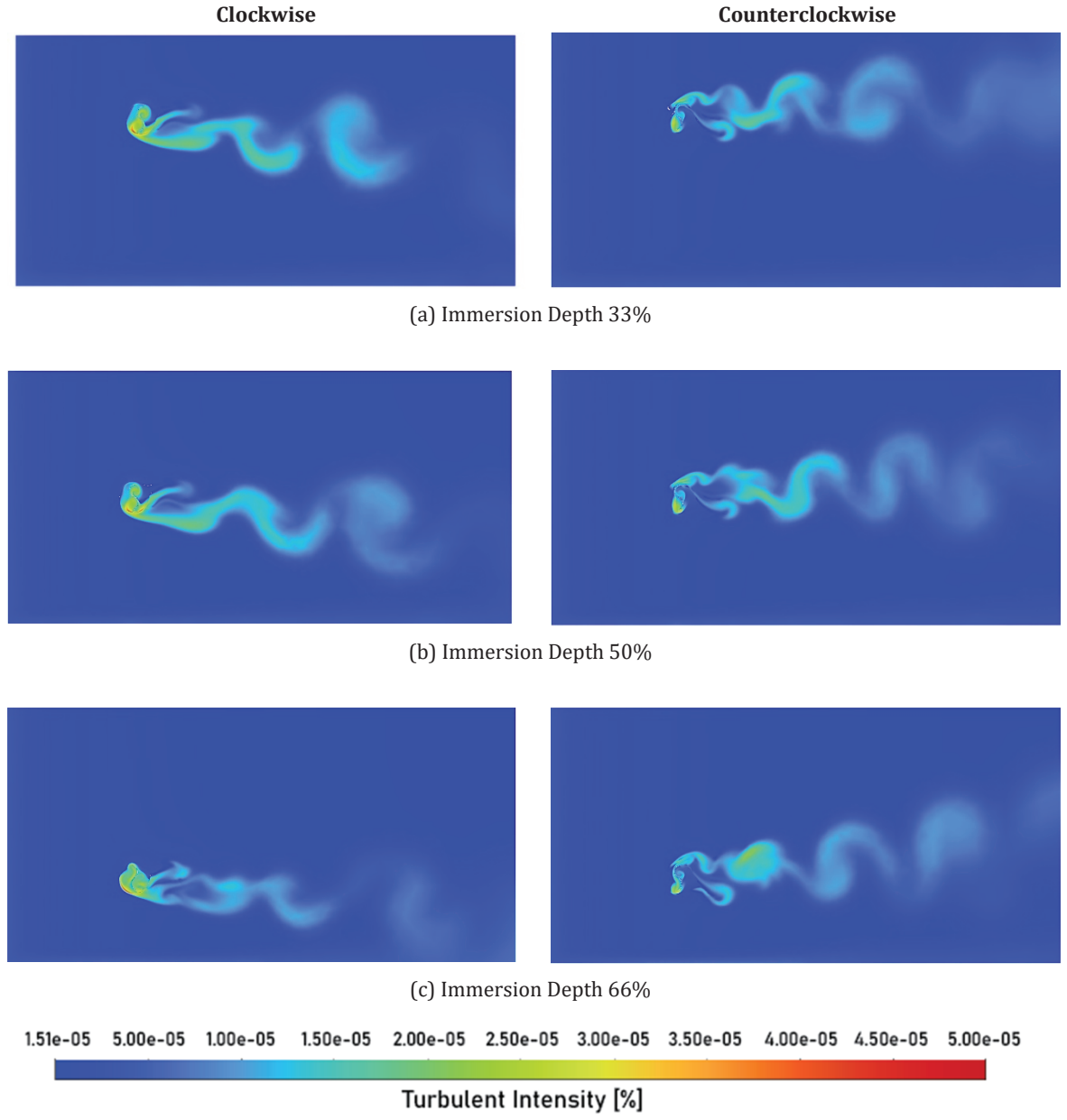

Figure 13 Contours of turbulent intensity in every depth immersion with different rotation direction variations.

The turbulence intensity contour in Figure 13 showed a similarity in the turbulence flow pattern across each variation applied. The similarity was found in the turbulence pattern, where the turbulence near the turbine was more concentrated with high intensity, and then the flow spread out and formed larger vortices behind the turbine, but with lower intensity. The difference was only in the direction of the turbulence flow. In the clockwise rotation direction, the vortices formed generally moved downward relative to the turbine, whereas in the counterclockwise rotation direction, the vortices formed generally moved upward relative to the turbine.

At a 66% immersion depth, the counterclockwise configuration showed a 6% decrease in maximum *Cp* at *TSR* 0.7. This decline might be attributed to the behavior of vortices formed around the turbine. In Figure 13 (c), where the turbine operated in a clockwise direction, the downward-directed vortices became constrained by the seabed. This limitation resulted in a more concentrated vortex intensity, reducing unwanted turbulence. Consequently, this increased flow stability could lead to more consistent water movement around the turbine. In contrast, the counterclockwise configuration did not experience this effect, as the turbulence expanded and led to greater instability.

With the results shown at the 66% variation, performance improvement continued when the deflector was applied. Deflectors can change the water flow pat-

terns around the turbine by increasing the flow speed on the forward beam and decreasing the rate of flow on the back beam. As a result of the negative torque on the reverse beam that was reduced. As demonstrated by Satrio et al. where the use of deflectors can improve the performance of turbines with an average increase of between 12% to 20% [25].

4 Conclusions

A numerical simulation of a cross-flow Savonius turbine for varying depth immersions and rotation directions has been carried out using CFD simulations. Savonius turbines with cross-flow configuration have excellent performance in operations under low *TSR* conditions, as evidenced by a decrease in maximum *Cp* values between 8% and 13% that increases as the *TSR* increases at all immersion depth variations. Turbine performance at low to medium *TSR* is closely related to the torque produced. This is demonstrated by achieving relatively higher *Cp* values than *Ct*, with an average difference of values between 11% and 26%. However, high *TSR* performance is greatly influenced by turbine RPM where the *Cp* value is tied to 7.97% below *Ct*.

In the application of immersion depth clockwise rotation of direction variations, variations with larger depths recorded the best results, i.e. 66% variations that consistently recorded the best results at both *Ct* and *Cp* values in all *TSR* conditions. This proves the proximity of interaction with the bottom surface has a good impact on Savonuis cross-flow turbines. In the application of the counterclockwise rotation of direction variation, the performance of the 33% variation improves by 6%, the same as the 50% variance increased by 4%. This is due to the direction of the vortex formed behind the turbine: in the clockwise rotation, the vortex tends to lead down, whereas in the counterclockwise rotation, the vortex tends to lead up.

Acknowledgments: The authors would like to convey their appreciation to Institut Teknologi Sepuluh Nopember (ITS), which funded the current project under a scheme called Collaborative Research Center of ITS under-contract number 1320/PKS/ITS/2024.

References

[1] IEA, "Oil 2023 Analisys and Forcast to 2028," *Int. Energy Agency*, 2023.

[2] I. Kurniawati, J. Pratilastiarso, and D. Satrio, "Analysis of the Effect of Cooling Water Condenser to Power Plant Cycle Using Cycle-Tempo Software," in *IES 2020 - International Electronics Symposium: The Role of Autonomous and Intelligent Systems for Human Life and Comfort*, Surabaya: IEEE, 2020, pp. 37–42. doi: https://doi.org/10.1109/IES50839.2020.9231722.

[3] M. N. Ariansyah, L. Diana, and D. Satrio, "Numerical Study the Effect of Gap Ratio on Flow Characteristics and Heat Transfer in Staggered Tube Banks," in *IOP Conference Series: Earth and Environmental Science*, Surabaya: IOP Publishing Ltd, 2022, p. 012065. doi: https://doi.org/10.1088/1755-1315/972/1/012065.

[4] D. Satrio *et al.*, "An Investigation on the Erosion Rate of Steam Turbine Blade with Variation of Material," *Int. Rev. Civ. Eng.*, vol. 14, no. 6, pp. 553–560, 2023, doi: 10.15866/irece.v14i6.22837.

[5] N. P. Purba *et al.*, "Suitable Locations of Ocean Renewable Energy (ORE) in Indonesia Region-GIS Approached," *Energy Procedia*, vol. 65, pp. 230–238, 2015, doi: 10.1016/j.egypro.2015.01.035.

[6] B. G. Marinus, J. Vercauteren, R. Vandenberghe, and J. Smeulders, "Laminar-Turbulent Transition on a Cambered NACA 16-009 Airfoil at Low Speed," *Int. Rev. Mech. Eng.*, vol. 14, no. June, pp. 351–359, 2020.

[7] B. K. Kirke and L. Lazauskas, "Limitations of fixed pitch Darrieus hydrokinetic turbines and the challenge of variable pitch," *Renew. Energy*, vol. 36, no. 3, pp. 893–897, 2011, doi: 10.1016/j.renene.2010.08.027.

[8] E. Erwandi *et al.*, "Numerical Analysis of Resistance and Motions on Trimaran Floating Platform for Tidal Current Power Plant," *Int. Rev. Model. Simulations*, vol. 17, no. 1, pp. 6–16, 2024, doi: 10.15866/iremos.v17i1.24366.

[9] C. Kang, F. Zhang, and X. Mao, "Comparison study of a vertical-axis spiral rotor and a conventional savonius rotor," *Asia-Pacific Power Energy Eng. Conf. APPEEC*, pp. 1–4, 2010, doi: 10.1109/APPEEC.2010.5448791.

[10] D. Satrio and I. K. A. P. Utama, "Experimental investigation into the improvement of self-starting capability of vertical-axis tidal current turbine," *Energy Reports*, vol. 7, pp. 4587–4594, 2021, doi: 10.1016/j.egyr.2021.07.027.

[11] D. Forbush, B. Polagye, J. Thomson, L. Kilcher, J. Donegan, and J. McEntee, "Performance characterization of a cross-flow hydrokinetic turbine in sheared inflow," *Int. J. Mar. Energy*, vol. 16, pp. 150–161, 2016, doi: 10.1016/j.ijome.2016.06.001.

[12] S. Bourget, O. Gauvin-Tremblay, and G. Dumas, "Hydrokinetic turbine array modeling for performance analysis and deployment optimization," *Trans. Can. Soc. Mech. Eng.*, vol. 42, no. 4, pp. 370–381, 2018, doi: 10.1139/tcsme-2017-0088.

[13] T. Ogawa and H. Yoshida, "The Effect of a Deflecting Plate and Rotot end Plates on performance of savonius-Type Wing Turbine," *Chem. Pharm. Bull.*, vol. 17, no. 11, pp. 1460–1462, 1994.

[14] L. Myers and A. S. Bahaj, "Wake studies of a 1/30th scale horizontal axis marine current turbine," *Ocean Eng.*, vol. 34, no. 5–6, pp. 758–762, 2007, doi: 10.1016/j.oceaneng.2006.04.013.

[15] B. Zhang, B. Li, C. Li, Y. Zhang, J. Lv, and H. Yu, "Effects of submergence depth on the performance of the savonius hydrokinetic turbine near a free surface," *Energy*, vol. 289, no. October 2023, p. 129899, 2024, doi: 10.1016/j.energy.2023.129899.

[16] J. Sarkar and S. Bhattacharyya, "Application of graphene and graphene-based materials in clean energy-related devices Minghui," *Arch. Thermodyn.*, vol. 33, no. 4, pp. 23–40, 2012, doi: 10.1002/er.

[17] M. A. Ramdhani and I. H. Cho, "Optimization of a Savonius hydrokinetic turbine for performance improvement: A comprehensive analysis of immersion depth and rotation direction," *Ocean Syst. Eng.*, vol. 14, no. 2, pp. 41–56, 2024, doi: 10.12989/ose.2024.14.2.041.

[18] K. Golecha, T. I. Eldho, and S. V. Prabhu, "Influence of the deflector plate on the performance of modified Savonius water turbine," *Appl. Energy*, vol. 88, no. 9, pp. 3207–3217, 2011, doi: 10.1016/j.apenergy.2011.03.025.

[19] EMEC, *Assessment of Tidal Energy Resource*. 2009.

[20] E. S. Hadi *et al.*, "Influence of the canal width and depth on the resistance of 750 DWT Perintis ship using CFD simulation," *Brodogradnja*, vol. 74, no. 1, pp. 117–144, 2023, doi: http://dx.doi.org/10.21278/brod74107.

[21] D. Satrio, Suntoyo, H. B. Widyawan, M. A. Ramadhani, and M. Muharja, "Effects of the distance ratio of circular flow disturbance on vertical-axis turbine performance: An experimental and numerical study," *Sustain. Energy Technol. Assessments*, vol. 63, no. March 2024, p. 103635, 2024, doi: 10.1016/j.seta.2024.103635.

[22] M. F. Ismail and K. Vijayaraghavan, "The effects of aerofoil profile modification on a vertical axis wind turbine performance," *Energy*, vol. 80, pp. 20–31, 2015, doi: 10.1016/j.energy.2014.11.034.

[23] P. Marsh, D. Ranmuthugala, I. Penesis, and G. Thomas, "The influence of turbulence model and two and three-dimensional domain selection on the simulated performance characteristics of vertical axis tidal turbines," *Renew. Energy*, vol. 105, pp. 106–116, 2017, doi: 10.1016/j.renene.2016.11.063.

[24] T. Maître, E. Amet, and C. Pellone, "Modeling of the flow in a Darrieus water turbine: Wall grid refinement analysis and comparison with experiments," *Renew. Energy*, vol. 51, pp. 497–512, 2013, doi: 10.1016/j.renene.2012.09.030.

[25] D. Satrio *et al.*, "The Influence of Deflector on the Performance of Cross-flow Savonius Turbine," *Int. Rev. Model. Simulations*, vol. 16, no. February, pp. 27–34, 2023, doi: 10.15866/iremos.v16i1.22763.

[26] M. Madi *et al.*, "Experimental Study on the Effect of Foil Guide Vane on the Performance of a Straight-Blade Vertical Axis Ocean Current Turbine," *Nase More*, vol. 71, 2024, doi: 10.17818/NM/2024/1.1.

[27] D. Satrio *et al.*, "The Advantages and Challenges of Carbon Fiber Reinforced Polymers for Tidal Current Turbine Systems - An Overview," in *IOP Conf. Series: Earth and Environmental Science*, Surabaya: IOP Publishing, 2024, p. 1298. doi: 10.1088/1755-1315/1298/1/012029.

[28] S. Musabikha *et al.*, "The effects of flow rate on impedance measurements of marine coatings using a rotating cylinder electrode," *J. Coatings Technol. Res.*, pp. 1–12, 2024, doi: 10.1007/s11998-024-00957-w.

[29] Rasgianti, Mukhtasor, and D. Satrio, "The Influence of Structural Parameters on the Ultimate Strength Capacity of a Designed Vertical Axis Turbine Blade for Ocean Current Power Generators," *Sustain.*, vol. 16, no. 7655, pp. 1–24, 2024, doi: https://doi.org/10.3390/su16177655.